Hindawi Publishing Corporation
Journal of Nanotechnology
Volume 2014, Article ID 683153, 10 pages
http://dx.doi.org/10.1155/2014/683153

Research Article

Cyclosporine A Loaded PLGA Nanoparticles for Dry Eye Disease: *In Vitro* Characterization Studies

Vijay D. Wagh and Dipak U. Apar

Department of Pharmaceutics, R. C. Patel Institute of Pharmaceutical Education and Research, Near Karwand Naka, Shirpur, Maharashtra 425405, India

Correspondence should be addressed to Vijay D. Wagh; drvijaydwagh@gmail.com

Received 26 July 2013; Revised 4 October 2013; Accepted 2 December 2013; Published 12 February 2014

Academic Editor: Joseph Irudayaraj

Dry eye disease is a common disease of the tear film caused by decreased tear production or increased evaporation. The objective of this study was to develop and evaluate poly (dl-lactide-co-glycolide) (PLGA) nanoparticles for CsA (CsA) ophthalmic delivery, for the treatment of dry eye disease. Topical CsA is currently the only and safe pharmacologic treatment of severe dry eye symptoms. Nanoparticles (NPs) were prepared by W/O solvent evaporation technique followed by probe sonicator and characterized for various properties such as particle size, entrapment efficiency, zeta potential, *in vitro* drug release, *in vitro* permeation studies by Franz diffusion cells, XRD, DSC, SEM, and stability studies. The developed nanosuspension showed a mean particle size in the range from 128 to 253.50 nm before freeze drying and after freeze drying 145.60 to 260.0 nm. The drug entrapment efficiency was from 58.35 to 95.69% and production yield was found between 52.29 ± 2.4 and 85.30 ± 2.1% in all preparations. The zeta potential of the Eudragit RL containing nanoparticles was positive, that is, 20.3 mV to 34.5 mV. The NPs formulations exhibited a biphasic drug release with initial burst followed by a very slow drug release and total cumulative release up to 24 h ranged from 69.83 to 91.92%. Kinetically, the release profiles of CsA from NPs appeared to fit best with the Higuchi model. The change of surface characteristics of NPs represents a useful approach for improvement of ocular retention and drug availability.

1. Introduction

Dry eye disease can also be known as Keratoconjunctivitis sicca, either due to insufficient tear production or excessive tear evaporation, both resulting in tears hyperosmolarity that leads to symptoms of discomfort and ocular damage. Dry eye disease is a prevalent disease that affects visual acuity, activities of daily living, and quality of life. Various environmental factors like contact lenses, pollution, working at video display terminals can affect the tear film and proceed up to infection, corneal ulcer, and blindness [1–6]. CsA is a well-known immunomodulatory agent that is commonly used to prevent rejection after organ/tissue transplantation [7]. It prevents T-cells from releasing cytokines (primarily interleukin-6) that incite the inflammatory component of dry eye [8–10].

Nanoparticles systems accelerate the drug penetration, increase corneal uptake, and avoid systemic absorption. It is able to deliver more intact drug at site of action as compared to free drug [11–13]. After administration, colloidal drug carriers can remain at the application site (*cul-de-sac*) and the prolonged release of the active ingredient starts by particle degradation or erosion, drug diffusion, or a combination of both, depending on the biodegradable or inert nature of the polymer [14]. Polymeric nanoparticle formulation is one of the strategies currently used to improve drug absorption across biological membranes [15]. Based on the literature data, the three most commonly used polymers in ophthalmic drug formulations are poly (alkyl cyanoacrylates), polycaprolactone, and poly (lactic acid)/poly(lactic-co-glycolic acid). Other polymers with ocular drug delivery application include chitosan, Eudragit RL/Eudragit RS, polystyrene, and

poly (acrylic acid). Much of the published data suggests that in the case of ophthalmic drug delivery, an appropriate particle size and a narrow size range, ensuring low irritation, adequate bioavailability, and compatibility with ocular tissues, should be sought for every suspended drug [16, 17].

The best known class of biodegradable polymers for sustained drug delivery is poly (dL-lactide-co-glycolide) (PLGA). PLGA is a biodegradable and biocompatible polymer that is hydrolytically degraded into nontoxic oligomer and monomer, lactic acid, and glycolic acid [18]. This is the reason that it has been used extensively in nanoparticulate drug delivery systems. Flurbiprofen-loaded PLGA nanoparticles were also studied extensively in various aspects for their application in ocular inflammation and proved to have good stability and ocular tolerance [19]. PLGA/Eudragit RL100 is a good nanovector for ophthalmic delivery and in past it was used for ciprofloxacin [20]. Based on these considerations, various strategies have been employed to modify NPs properties, including the use of cationic or biodegradable polymers. We have evaluated the particle formation process of the NPs prepared from PLGA polymers with the benefit of positively charged polymers, Eudragit RL100 in different ratios, which could interact with the anionic mucins present in the mucus layer at the surface of the eye [21]. The current study aimed at developing and optimizing a polymeric nanoparticulate formulation of CsA for ocular delivery to improve corneal uptake efficiency to treat dry eye disease using design of experiments by employing 3-level full factorial design (design-Expert software, version 8; Stat-Ease, Inc., Minneapolis, Minnesota, USA).

2. Material and Methods

2.1. Material. The poly(lactic-co-glycolic acid) (PLGA) polymer Resomer RG 503 was obtained from Sigma Aldrich Pvt. Ltd, Mumbai, India and Eudragit RL100 from Evonic degusa, Mumbai, India. Cyclosporine *A* was a gift from Alkem Pvt. Ltd. (India). Poly (vinyl alcohol) (PVA) (MW 30,000–70,000) was supplied by Hi-Media Lab. Pvt. Ltd. Mumbai, India. D-mannitol, Dichloromethane, and acetonitrile (HPLC grade) HPLC grade solvents were purchased from E. Merck (India) Ltd. All other solvents and materials used were of analytical grade.

2.2. Methods

2.2.1. Preparation of Buffer Solutions. The composition of simulated fluid (SLF), pH 7.4, was 8.3 g of NaCl, 0.084 g of $CaCl_2 \cdot 2H_2O$, and 1.4 g of KCl in 1 litre of ultraPurified water [22].

Composition of Phosphate-Buffer Saline (PBS), pH 7.4. PBS was disodium hydrogen phosphate 1.38 g of potassium dihydrogen phosphate 0.19 g and sodium chloride 8.0 g, in 1 litre of ultra purified water [23].

Table 1: Factorial design parameters and experimental condition.

Factors	Levels used, Actual (coded)		
	Low (−1)	Medium (1)	High (+1)
A = polymer PLGA (mg)	25	50	75
B = Eudragit RL100 (mg)	25	50	75

2.2.2. Preparation of CsA Loaded PLGA NPs. Polymeric nanoparticle can be prepared in several ways. The formulations of drug loaded nanoparticles were done with solvent evaporation (o/w emulsification) followed by lyophilization, [24, 25]. CsA loaded nanoparticles F1–F9 were prepared using PLGA and Eudragit RL100 in three different polymer ratios. PLGA and/or Eudragit RL100 (50 mg) was dissolved in 3 mL dichloromethane with CsA (10 mg). This organic mixture was then emulsified in 10 mL of an aqueous PVA solution (1% w/v) by sonication (amplitude 20%, 6 min) using an ultrasound probe (PCI analytics Ltd., India.) in an ice bath. This emulsion was then diluted in 40 mL of PVA stabilizer solution (0.36% w/v). The organic solvent was allowed to evaporate at room temperature under magnetic stirrer (700 rpm), for 4 hour at room temperature (Remi Instruments Ltd., Mumbai, India). The nanosuspension was then resuspended in mannitol solution (5% w/v). The resulting nanosuspension was subsequently cooled down to −20°C and freeze-dried (Benchtop freeze dryer, Virtis Ltd. USA).

2.2.3. Experimental Design. The design of experiments (DOE) technique was used to provide an efficient means to optimize the polymer concentrations. DOE is an approach for effectively and efficiently exploring the cause and effect relationship between process variables and the output. *A* 2-factor 3-level factorial central composite experimental design technique was employed to investigate the variables. This technique was applied to quantify the influence of operating parameters on the particle size and entrapment efficiency of nanoparticles. The dependant variables were polymer PLGA and Eudragit RL100 concentrations. The factorial design parameters and experimental condition are shown in Table 1. The goal of the experimental design was to find out, with the minimum number of experimental runs, which process variables have the biggest impact on the final product. Various batches of CsA loaded nanoparticle were prepared based on the 3^2 factorial designs. The independent variables were polymer PLGA concentrations 25 to 75 mg (*A*) and Eudragit RL100 25 to 75 mg (*B*) and their levels are shown in Table 1.

2.2.4. Characterization of Nanoparticle

(1) Production Yield. The production yields were calculated as the weight percentage of the final product after drying, with respect to the initial total amount of CsA and polymer used for the preparations. The yield of NPs (1) was calculated as indicated below:

$$\%\text{Yield} = \frac{\text{Total weight of obtained NPs (mg)}}{\text{Drug + polymer weight (mg)}} \times 100. \quad (1)$$

(2) Particle Size Analysis. The particle size and polydispersity index (PDI) of NPs were measured using dynamic light scattering (Zetasizer Nano ZS 90, Malvern Ltd., UK). Dynamic light scattering (also known as PCS-Photon Correlation Spectroscopy) measures Brownian motion and relates this to the size of the particles. It does this by illuminating the particles with a laser and analysing the intensity fluctuations in the scattered light. All samples were diluted in a 1 : 10 ratio with deionised water to get optimum 100–200 kilo counts per second (KCPS) for measurements. The mean particle size of each sample was determined three times ($n = 3$).

(3) Zeta Potential. The zeta potential of the particles were determined by electrophoretic light scattering (Zetasizer Nano ZS 90, Malvern Ltd., UK). NPs were suspended either in simulated lacrimal fluid (SLF) or Ultrapurified water (UPW). The average values of three separate determinations.

(4) Entrapment Efficiency. The drug content in NPs was determined directly by measuring the encapsulated CsA amount in NPs. *A* known weight of freeze-dried powder was dissolved in acetonitrile : water (7 : 3) solution and put for 1 h in an ultrasonic bath. After centrifugation for 30 min at 14,000 rpm by using cooling centrifuge (Remi Instruments Ltd. Mumbai, India). CsA content of the samples was determined by HPLC (Agilent). *A* Phenomenex-Luna C18 column (250 × 4.60 mm) was used. The mobile phase consisted of a 70 : 30 (v/v) mixture of acetonitrile: water [26]. It was detected at 204 nm with the flow rate of 1 mL/min. Entrapment efficiency of the CsA (2) was calculated as indicated below:

$$\%\ \text{E.E} = \frac{\text{Weight of drug determined (mg)}}{\text{Weight of drug added}} \times 100. \quad (2)$$

(5) In Vitro Drug Release Studies. The freeze-dried NPs containing 100 μg CsA were suspended in vials containing 30 mL SLF and incubated in a water bath at 32°C which is the temperature of the eye surface, using continuous magnetic stirrer at 200 rpm. At given time intervals 1 mL samples were withdrawn, centrifuged for 30 min at 14,000 rpm, and the amount of CsA in the samples was determined by HPLC method as described before. Various mathematical equations were applied to define the kinetics of the drug release. The best curve fit of the release data was tested with the mathematical models of zero and first order, Higuchi, and korsmayer kinetics [22].

(6) In Vitro Permeation Studies. The permeation studies [27] were performed using Franz diffusion cells with a diffusion area of 2.26 cm^2. Sigma dialysis membrane having a molecular weight cutoff of 12,400 Da was used. Membranes were soaked in UPW for 24 h before mounting in Franz diffusion cell. The SLF in the thermostated (32°C) receptor chamber was stirred at 200 rpm. An amount of NPs containing 50 μg CsA was dispersed in 5 mL UPW and gently placed into the donor chamber. At specified time intervals, 1 mL samples were withdrawn for HPLC determination and replaced immediately with an equal volume of SLF solution.

(7) Morphology of NPs. The surface morphology of the optimized formulations (F3) was studied using a scanning electron microscope (JSM 6390, JEOL) operated at an accelerating voltage of 10 kV.

(8) Thermal Analysis. The thermal behaviour of pure drug, freeze dried drug loaded NPs, and freeze dried blank nanoparticles was conducted using differential scanning calorimeter (Mettler Toledo, Switzerland) at a heating rate of 10°C/min. The measurements were performed at a heating range of 30 to 300°C under nitrogen atmospheres.

(9) X-Ray Diffraction (Xrd) Studies. X-ray diffractogram of the plane drug, blank microsphere, and drug-loaded nanoparticle was recorded by a diffractogram (Brucker AXS D8 Advance) using Cu-Ka line as a source of radiation which was operated at the voltage 40 kV and the current 35 mA. All samples were measured in the 2θ angle range between 3 and 80° and 0.020° step size.

(10) Accelerated Stability Studies. The NPS formulation (optimized batch F3) was utilized for carrying out accelerated stability studies according to International Conference on Harmonisation (ICH) Q1A (R^2) guidelines [28]. For the products stored in refrigerator ICH guidelines suggested long term stability at 25°C ± 3°C and accelerated stability study at 25°C ± 2°C/60% RH ± 5% RH (relative 10 humidity). Accelerated stability study was performed with the prime aim to assess the stability of NPs at 25 ± 2°C/60 ± 5% RH with respect to particle size and entrapment efficiency.

Freshly prepared NPs were filled in 3 different amber coloured glass vials, sealed, and placed in stability chamber (CHM-10S, Remi Instruments. Ltd. Mumbai, India) maintained at 25 ± 2°C/60 ± 5% RH for a period of total 3 months. The dried powder samples subjected for stability test were redispersed in distilled water and analyzed with a sampling interval of 1 month for particle size and EE of the CsA-NPs over 3-month period.

3. Results and Discussion

The solvent evaporation method described here appeared to be a suitable and simple technique to prepare PLGA containing NPs loaded with CsA. It is a one-step process, easy, and rapid.

3.1. Formulation of Nanoparticles. Nine formulations of CsA loaded nanoparticle were prepared by emulsification solvent evaporation using factorial design, in which the independent variables were polymer concentrations PLGA 25 to 75 mg (A) and Eudragit RL100 25 to 75 mg (B) (Table 5) and particle size (nm) of the nanoparticle (X_1) and Zeta potential (X_2) were taken as response parameters as the dependent variables.

3.2. Optimization Data Analysis and Model Validation

Optimization Validation to the Model. The two factors with lower, middle, and upper design points in coded and uncoded

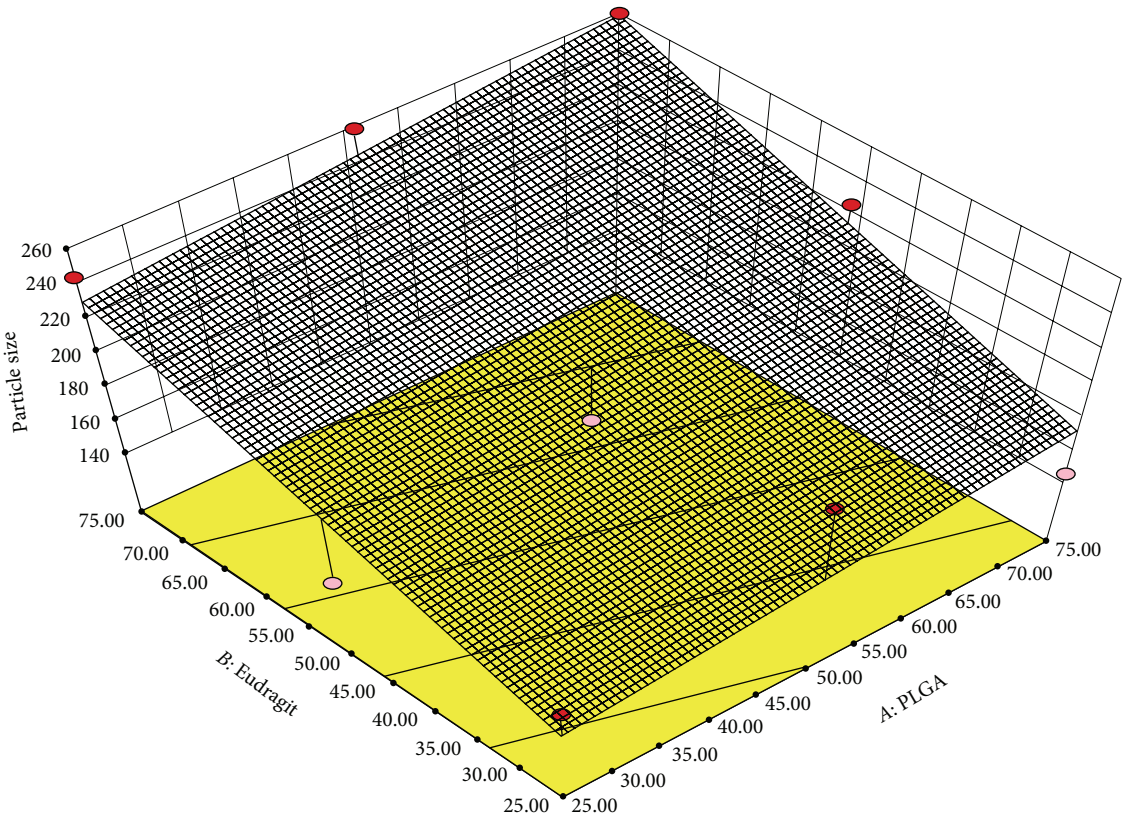

Figure 1: Response surface plots for the A and B on particle size (X_1), where A = PLGA concentration and B = Eudragit RL100 concentration.

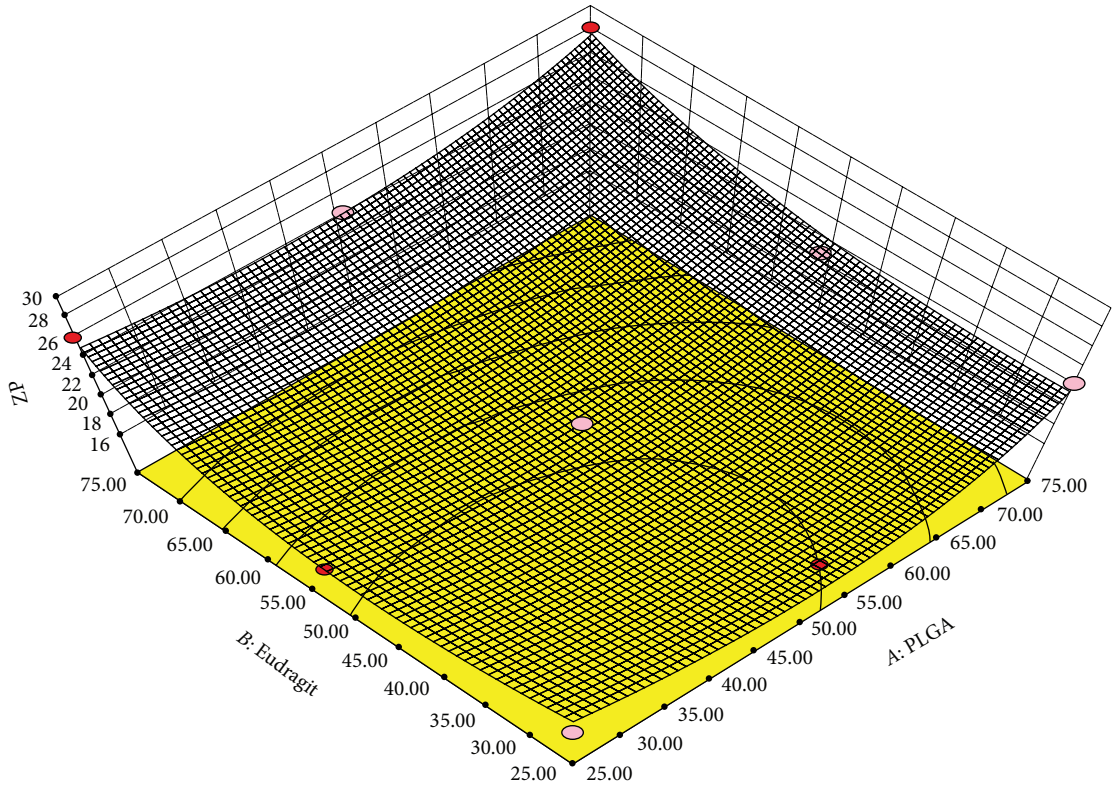

Figure 2: Response surface plots for the A and B on zeta potential (X_2), where A PLGA concentration and B Eudragit RL100 concentration.

values are shown in Table 1. The ranges of responses A and B were 145.5 ± 12 to 260.0 ± 26 nm and +20.3 ± 6.4 to +34.5 ± 4.8 mV, respectively. All the responses observed for nine formulations prepared were fitted to various models using Design-Expert software. It was observed that the best-fitted models were linear for particle size and quadratic for Zeta potential. The values of R^2, adjusted R^2, predicted R^2, Standard deviation (SD), and % coefficient variation (% CV) are given in Table 2, along with the regression equation generated for each response. The results of ANOVA in Table 3, for the dependent variables, demonstrate that the model was significant for both response variables.

It was observed that independent variables A (polymer concentrations PLGA) and B (polymer concentrations Eudragit RL100) had a positive effect on particle size (X_1) and Zeta potential (X_2).

Regression Equations of the Fitted Linear and Quadratic Model. Consider the following:

$$X_1 = 201.78 + 13.52 * A + 41.87 * B$$
$$X_2 = 17.76 + 1.78 * A + 3.55 * B - 0.97 * A * B + 2.02 * A_2 + 3.62 * B_2. \quad (3)$$

The coefficients with more than one-factor term in the regression equation represent interaction terms. It also shows that the relationship between factors and responses is not always linear. When more than one factor is changed simultaneously and used at different levels in a formulation, a factor can produce different degrees of response. The interaction effects of A and B were favorable (positive) for responses X_1 and X_2.

Response Surface Plot Analysis. Three-dimensional response surface plots generated by the Design Expert software are presented in Figures 1 and 2 for the studied responses, that is, particle size and zeta potential. Figure 1 depicts response surface plot of polymer concentrations PLGA (A) and Eudragit RL100 (B) on particle size, which indicate that A and B show linear effect; that is, when increased from low to high the value of particle size was also increased. Figure 2 represents response surface plot of the effect of polymer concentrations PLGA (A) and Eudragit RL100 (B) on Zeta potential which indicates a quadratic effect. This explains that the higher the amount of polymer, the more will be the zeta potential because of the more availability of polymer Eudragit RL100 to give the positive charge in formulation.

Optimization and Validation. A numerical optimization technique by the desirability approach was used to generate the optimum settings for the formulation. The process was optimized for the dependent variables such as particle size (X_1) and Zeta potential (X_2). The optimum formulation was selected based on the criteria of attaining the minimum value of particle size with considerable Zeta potential. Formulation F3 containing % polymer concentrations PLGA and Eudragit RL100 fulfilled all the criteria set from desirability search. The reliability of the response surface model, a new optimized formulation, was prepared according to the predicted model and evaluated for the responses.

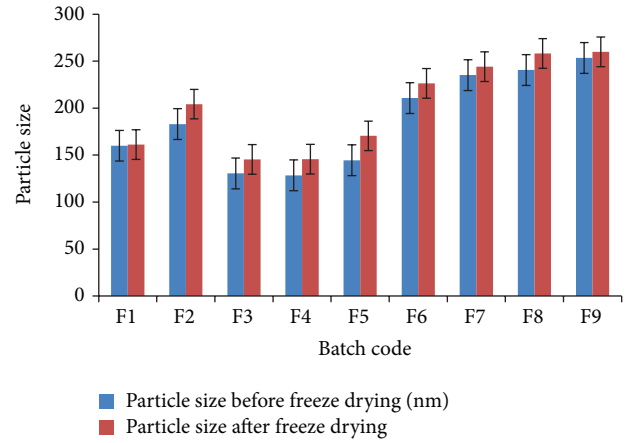

Figure 3: Effect of polymer concentration on particle size.

3.3. Characterization of Nanoparticle

3.3.1. Production Yield of NPs. The yield of production was found in the range between 52.29 and 85.30% (Table 4). The production yield was obtained in PLGA and Eudragit RL NPs. Because CsA is a very poorly water soluble drug, it was partitioned in the organic phase of the initial emulsion and consequently, very little amount of drug was lost to the aqueous phase [23].

3.3.2. Particle Size Analysis. The major objective of using general optimal design was to determine the levels of the two factors, that is, PLGA concentrations and Eudragit RL100 concentrations, which produce the NPs with minimum particle size. Particle size and Polydispersity index (PDI) of the fabricated batches were in the range of 128.48 to 253.50 nm and 0.22 to 0.669 before freeze drying and after freeze drying were 145.60 to 260.0 and 0.105 to 0.404, respectively, (Table 4). Particle size distributions of all preparations are homogenous and well suited for ocular use. The particle size for ophthalmic applications should not exceed 10 μm to prevent scratching and foreign body sensation [11].

Effect of Polymer Concentrations on the Particle Size. Different polymer concentrations have shown very predominant effect on the particle size of the CsA loaded NPs. Figure 3 clearly represents that the particle size was decreasing or increasing with Eudragit RL100 concentrations, due to the physicochemical properties of the polymer. Particle size decrease can be attributed to the fact that the viscosity of the internal phase of the emulsion may also be changed regarding to the polymer type used. An increase in viscosity of internal phase leads to an increase in size of the particles under a constant sonication input. During the formation of NPs prepared by mixture of PLGA-Eudragit RL100 (25 : 25, 25 : 50, 25 : 75), the viscosity of the internal phase of the emulsion might be lower than other polymer compositions. The results obtained correlated well with previous studies and investigated the influence of Eudragit RL100 and PLGA polymers on NPs size [29].

Table 2: Summary of results of regression analysis for responses X_1 and X_2.

Models	R^2	Adjusted R^2	Predicted R^2	SD	% CV
Response (X_1)linear	0.6485	**0.5313**	**0.2736**	32.39	**13008.71**
Response (X_2) quadratic	**0.9800**	**0.9466**	**0.7560**	**0.95**	**33.07**

Table 3: Results of analysis of variance for particle size.

Parameters	DF*	SS*	MS*	F^*	Significance of P
Particle size					
Model	2	1161.1	5806.5	5.53	0.0434 significant
Residual	6	6295.87	1049.3	—	—
Total	8	17908.98	—	—	—
Zeta potential					
Model	5	132.79	26.56	29.34	0.0095 significant
Residual	3	2.72	0.91	—	—
Total	8	135.51	—	—	—

Where, DF* indicates degrees of freedom; SS* sum of square; MS* mean sum of square and F^* is Fischer's ratio.

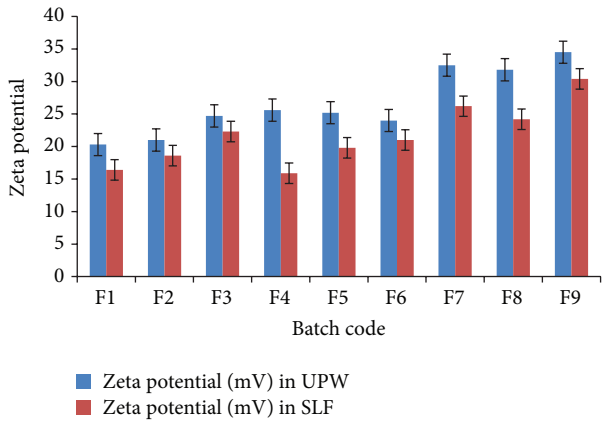

Figure 4: Zeta potential of different batches of CsA-NPs in UPW and SLF.

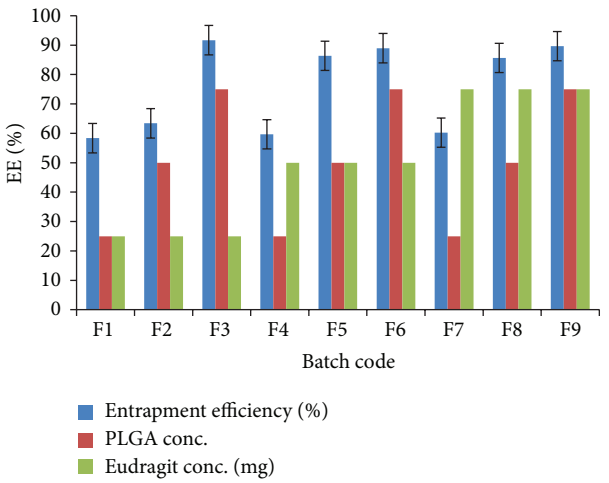

Figure 5: Effect of polymer concentration on percent entrapment efficiency.

3.3.3. Zeta Potential. Zeta potential measurement is an adequate method in order to evaluate NPs surface properties and to detect any eventual modification after freeze drying. The zeta potential values were found to be 20.3 to 34.5 mV dependent on the polymer type used (Table 5 and Figure 4). The zeta-potential of nanoparticles was found to possess positive surface charges due to the positively charged Eudragit RL100. The surface charges of the NPs prepared by PLGA-Eudragit RL100 mixtures were positive. The charge ratios were not related to Eudragit RL100 ratios, because only a small amount of amphiphilic Eudragit molecules are needed to obtain a positive charge at the particle surface. Same results were obtained in the studies of [30]. It is important to use positively charged NPs since it will prolong the residence time of the formulation in the precorneal area, because of interactions with negatively charged mucins. The zeta potential of the NPs was measured in UPW in both before and after lyophilization. The absolute zeta potential values of the NPs were reduced in after lyophilization compared to before lyophilization.

3.3.4. Entrapment Efficiency. Nine different batches of nanoparticles were prepared by varying the polymer concentrations. The amount of drug was kept constant for all the batches. The entrapment efficiency of the CsA loaded NPs is shown in Table 5. The entrapment efficiency and percent of all the nine batches range from 58.35 to 91.69%. The reason of low production yield may be loss of water soluble coating polymer from the surface during washing procedure. Such high value of entrapment efficiency may be due to the hydrophobic character of CsA; high entrapped efficiency and production yield was obtained in PLGA and Eudragit RL NPs. Because CsA is a very poorly water soluble drug, it was partitioned in the organic phase of the initial emulsion and consequently, very little amount of drug was lost to the aqueous phase [23].

Effect of Polymer Concentration on Entrapment Efficiency. CsA is a highly lipophilic or water insoluble drug which belongs to BCS class II. Thus, it is very well soluble in different organic solvent. In the present study, as the PLGA polymer concentrations increased (25 mg to 75 mg) the entrapment efficiency of the drug CsA is also increased (Figure 5).

Table 4: Particle size, PDI of CsA loaded NPs after and before freeze drying (FD) and production yield of NPs.

NPs code	Particle size before FD (nm)	Polydispersity index (PDI) before FD	Particle size after FD (nm)	Polydispersity index (PDI) after FD	Production yeild
F1	160.0 ± 08	0.395 ± 0.061	161.20 ± 10	0.640 ± 0.053	52.29 ± 2.4
F2	182.98 ± 13	0.265 ± 0.084	204.30 ± 12	0.460 ± 0.081	55.72 ± 3.1
F3	130.5 ± 10	0.105 ± 0.042	145.5 ± 12	0.262 ± 0.054	85.30 ± 2.1
F4	128.48 ± 13	0.388 ± 0.060	145.7 ± 13	0.582 ± 0.065	64.90 ± 3.0
F5	144.53 ± 13	0.208 ± 0.045	170.5 ± 14.5	0.508 ± 0.051	80.45 ± 2.6
F6	210.75 ± 16	0.458 ± 0.043	226.3 ± 18	0.655 ± 0.048	81.90 ± 1.9
F7	235.2 ± 19.5	0.198 ± 0.058	244.1 ± 23	0.669 ± 0.063	56.87 ± 2.8
F8	240.68 ± 22	0.410 ± 0.063	258.3 ± 24.5	0.620 ± 0.058	80.39 ± 2.5
F9	253.50 ± 18	0.404 ± 0.057	260.0 ± 26	0.474 ± 0.066	83.40 ± 2.8

Data as mean ± SD, $n = 3$, *FD: Freeze drying.

Table 5: Zeta potential and percent entrapment efficiency of different PLGA loaded NPs.

NPs Code	Factor A	Factor B	Zeta potential (mV) in UPW	Zeta potential (mV) in SLF	Entrapment efficiency (% E.E)
F1	25	25	+20.3 ± 6.4	+16.4 ± 5.2	58.35 ± 2.4
F2	50	25	+21.0 ± 2.3	+18.6 ± 2.1	63.41 ± 3.2
F3	75	25	+24.7 ± 1.5	+22.3 ± 1.4	91.69 ± 1.4
F4	25	50	+25.6 ± 3.2	+15.9 ± 3.7	59.65 ± 2.3
F5	50	50	+25.2 ± 4.7	+19.8 ± 4.3	86.37 ± 1.7
F6	75	50	+24.0 ± 5.0	+21.0 ± 4.8	88.96 ± 1.73
F7	25	75	+32.5 ± 5.4	+26.2 ± 5.3	60.21 ± 3.4
F8	50	75	+31.8 ± 5.9	+24.2 ± 6.0	85.66 ± 2.72
F9	75	75	+34.5 ± 4.8	+30.4 ± 5.9	89.65 ± 2.6

Data as mean ± SD, $n = 3$.

This can be explained on the basis that higher amount of polymeric phase is available for the dissolution of the CsA.

3.3.5. In Vitro Drug Release Studies. *In vitro* drug release profile of CsA loaded NPs showed biphasic release pattern by an initial burst release that was observed (Figure 6). This might be a result of the internal structure of NPs gained by freeze drying and lyophilization procedures as reported by other authors [31, 32].

In this study, another reason of high burst might be the result of crystal structure of CsA being transformed to an amorphous structure after the lyophilization process. Formation of amorphous structure from crystal may lead to an increase in CsA solubility. During preparation of NPs, CsA could precipitate as amorphous substance in the PLGA matrix. After the initial burst effect, the drug was released slowly.

In vitro release of CsA loaded NPs was studied up to 24 hrs in 7.4 pH phosphate buffer medium. For all the nine batches, about 40% of drug was released within 6 hours and total cumulative release within 24 h was found between 70% and 90% for all formulations. Low aqueous solubility may be a reason for the slow release of CsA from the polymer matrices after burst release. On the other hand, the increase in PLGA concentrations prolonged the CsA release from NP.

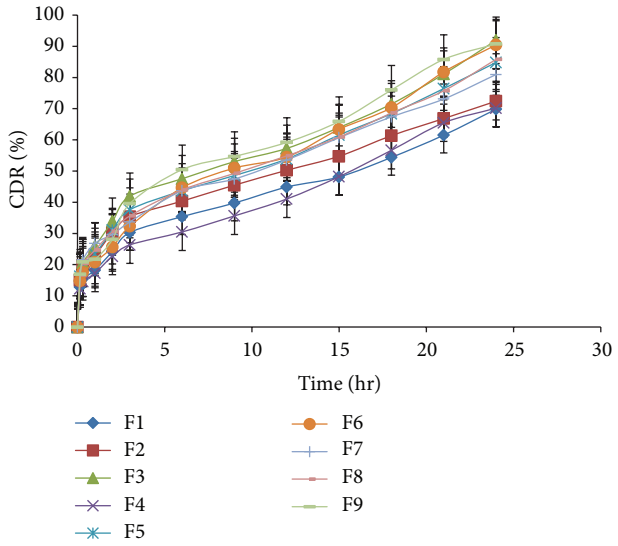

Figure 6: *In vitro* drug release study of CsA loaded NPs.

Table 6: Model fitting of the release profile using four different models.

Batch code	Coefficient of determination (R^2)			Best fit model
	Zero order	First order	Higuchi	
F3	**0.909**	**0.893**	**0.974**	Higuchi
	Korsmeyer Peppa's equation			
	R^2	K value	N value	Mechanism
F3	**0.977**	**0.316**	**0.508**	Quasi fickian

The bold values refer to coefficient of variation and its correct according to given headings.

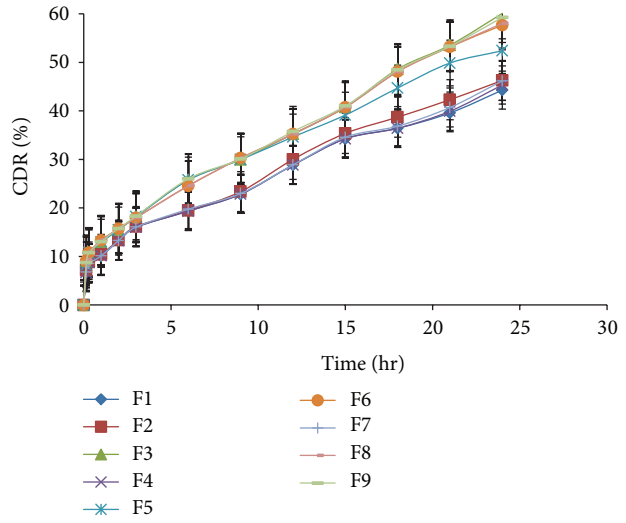

Figure 7: *In vitro* permeation profile of CsA-NPs of all nine batches.

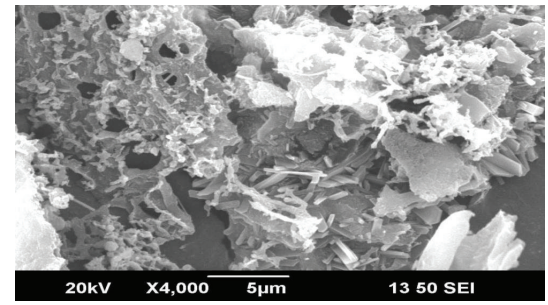

Figure 8: SEM image of optimized formulation (F3).

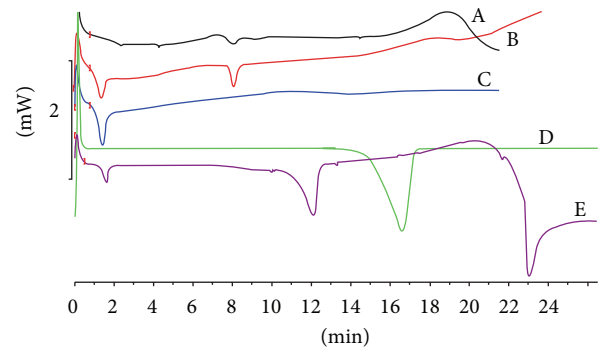

Figure 9: DSC thermogram of A-Cyclosporine, B-Cyclosporine with PLGA, C-PLGA, D-Eudragit RL100, and E-NPs optimized batch F3 (CsA P75-E25).

Drug Release Kinetics. The release constant was calculated from the slope of the appropriate plots and the regression coefficient (R^2) was determined. It was found that the *in vitro* drug release of F3 formulations was best explained by Higuchi kinetic, matrix diffusion mechanism, as the plots showed the highest linearity, $R^2 = 0.974$ (Table 6). The corresponding plot of log cumulative percentage drug release versus log time of the Korsmeyer-Peppas equation indicated a good linearity of regression coefficient (R^2), 0.977 indicating that optimized formulation (F3) followed quasi fickian transport, which is the drug transport mechanism.

3.3.6. In Vitro Permeation Studies. Franz diffusion cell study aimed to obtain the preinformation about *in vivo* studies by using cellulose membrane simulating human cornea. No significant difference in release and diffusion through the membrane was observed between the developed NPs formulations (Figure 7). The cumulative percentage of CsA in receptor compartment was between 44 and 60% for all formulations at the end of 24 h.

3.3.7. Morphology of NPs. The morphology of the optimized formulation (F3) nanoparticles was examined by scanning electron microscopy (Figure 8). Nanoparticles are spherical in shape and possessed a smooth surface and also they had no rupture on the surface; such morphology would result in slow clearance and good deposition pattern in ocular cavity [33, 34].

3.3.8. Thermal Analysis. The thermogram of CsA exhibited a sharp endothermic peak at 115.15°C, indicated melting point which was reported in the literature. Characteristic peak of CsA disappeared in the drug loaded nanoparticles. DSC studies revealed that CsA was molecularly dispersed inside the nanoparticle (Figure 9).

3.3.9. X-Ray Diffraction (XRD) Studies. The X-ray diffraction spectra were recorded for CsA, blank nanoparticle and drug loaded nanoparticle for investigating the crystallinity of the drug in the polymeric nanoparticle (Figure 10). CsA X-ray diffractogram illustrates the crystalline nature of drug. In contrast, the blank and drug loaded nanoparticle that

Table 7: Stability characteristics of cyclosporine loaded NPs in terms of mean particle size and zeta potential.

Stability parameter	Test period			
	0 month	1 month	2 months	3 months
Particle size (nm)	145.5 ± 12	147.87 ± 6.89	148.17 ± 9.28	148.56 ± 7.80
Zeta potential	+22.3 ± 1.4	+21.0 ± 1.0	+20.3 ± 0.9	+19.8 ± 1.6

Data as mean (mean ± SD, $n = 3$).

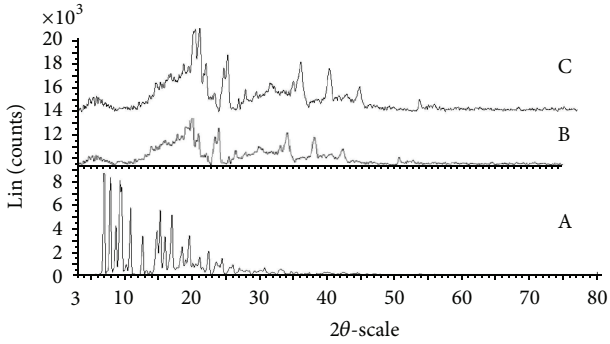

Figure 10: A-Cyclosporine, B-blank nanoparticles, and C-drug loaded nanoparticles.

produces peaks with low intensity indicates an almost amorphous state of these polymers. The absence of crystalline peaks of CsA *A* in drug loaded nanoparticle indicates that the drug was molecularly dispersed in the polymer and conversion of crystalline form of drug into the amorphous after freeze drying.

3.3.10. Accelerated Stability Studies. Particle size and Zeta potential variations during 3 months of storage were assessed. Respective data are given in Table 7. The particle size was increased slightly from 147.87 ± 6.89 nm to 148.56 ± 7.80 nm during stability studies. The zeta potential of the optimized batch after 3 months (+21.0 ± 1.0 to +19.8 ± 1.6 mV) indicated that the drug was retained within the nanoparticles throughout the stability period. The obtained results showed that there was no significant change in the mean particle size and zeta potential. There was a very slight decrease of the drug loading which may be due to the expulsion of drug from polymer matrix during storage.

4. Conclusion

The present study reports the preparation and physicochemical characterization of CsA NPs which combine the PLGA with the positively charged properties of Eudragit RL100. The results indicate that both the mean diameter and the surface charge on NPs were markedly affected by the polymer type. The PLGA, Eudragit RL100-CsA (75 : 25 or Batch F3) NPs, showed small particle size and positive surface charge, which makes them suitable for ocular use. In conclusion, we have demonstrated that NPs with different properties could modulate the drug release in the *cul-de-sac* or in the ocular tissues after uptake by epithelial cells. The system interacts with eye surface, ensuring optimal contact between the formulation and the mucosa. It provides sustained drug release in the *cul-de-sac* for an extended period of time. These results indicate that CsA loaded NPs have great potential as drug delivery systems and are promising formulations in the management of dry eye disease.

Conflict of Interests

None of the authors have any financial and personal relationships with other people or organizations that could inappropriately influence (bias) their work.

References

[1] V. D. Wagh, D. U. Apar, and S. J. Surana, "Drug delivery and pharmacotherapy for dry eye disease," *International Journal of Pharmacy and Pharmaceutical Sciences*, vol. 4, no. 2, pp. 42–46, 2012.

[2] V. D. Wagh, D. U. Apar, and S. J. Surana, "Animal models of dry eye disease: a review," *Journal of Pharmaceutical Sciences and Research*, vol. 4, no. 3, pp. 1758–1760, 2012.

[3] S. C. Pflugfelder, "Antiinflammatory therapy for dry eye," *The American Journal of Ophthalmology*, vol. 137, no. 2, pp. 337–342, 2004.

[4] S. C. Pflugfelder, A. Solomon, and M. E. Stern, "The diagnosis and management of dry eye: a twenty-five-year review," *Cornea*, vol. 19, no. 5, pp. 644–649, 2000.

[5] M. E. Stern, J. Gao, K. F. Siemasko, R. W. Beuerman, and S. C. Pflugfelder, "The role of the lacrimal functional unit in the pathophysiology of dry eye," *Experimental Eye Research*, vol. 78, no. 3, pp. 409–416, 2004.

[6] A. Behrens, J. J. Doyle, L. Stern et al., "Dysfunctional tear syndrome: a Delphi approach to treatment recommendations," *Cornea*, vol. 25, no. 8, pp. 900–907, 2006.

[7] Q. Zu, S. P. Kambhampati, and R. M. Kannan, "Nanotechnology approaches for ocular drug delivery," *Middle East African Journal of Ophthalmology*, vol. 20, no. 1, pp. 26–37, 2013.

[8] E. McCabe and S. Narayanan, "Advancements in anti-inflammatory therapy for dry eye syndrome," *Optometry*, vol. 80, no. 10, pp. 555–566, 2009.

[9] M. W. Belin, C. S. Bouchard, and T. M. Phillips, "Update on topical cyclosporin A: background, immunology, and pharmacology," *Cornea*, vol. 9, no. 3, pp. 184–195, 1990.

[10] S. L. Schreiber and G. R. Crabtree, "The mechanism of action of cyclosporin A and FK506," *Immunology Today*, vol. 13, no. 4, pp. 136–142, 1992.

[11] R. C. Mundargi, V. R. Babu, V. Rangaswamy, P. Patel, and T. M. Aminabhavi, "Nano/micro technologies for delivering macromolecular therapeutics using poly(D,L-lactide-co-glycolide) and its derivatives," *Journal of Controlled Release*, vol. 125, no. 3, pp. 193–209, 2008.

[12] K. Chaturvedi, K. Ganguly, A. R. Kulkarni et al., "Cyclodextrin-based siRNA delivery nanocarriers: a state-of-the-art review," *Expert Opinion on Drug Delivery*, vol. 8, no. 11, pp. 1455–1468, 2011.

[13] P. Calvo, C. Thomas, M. J. Alonso, J. L. Vila-Jato, and J. R. Robinson, "Study of the mechanism of interaction of poly(ε-caprolactone) nanocapsules with the cornea by confocal laser scanning microscopy," *International Journal of Pharmaceutics*, vol. 103, no. 3, pp. 283–291, 1994.

[14] K. S. Soppimath, T. M. Aminabhavi, A. R. Kulkarni, and W. E. Rudzinski, "Biodegradable polymeric nanoparticles as drug delivery devices," *Journal of Controlled Release*, vol. 70, no. 1-2, pp. 1–20, 2001.

[15] R. M. Mainardes, M. C. C. Urban, P. O. Cinto et al., "Colloidal carriers for ophthalmic drug delivery," *Current Drug Targets*, vol. 6, no. 3, pp. 363–371, 2005.

[16] A. S. Guinedi, N. D. Mortada, S. Mansour, and R. M. Hathout, "Preparation and evaluation of reverse-phase evaporation and multilamellar niosomes as ophthalmic carriers of acetazolamide," *International Journal of Pharmaceutics*, vol. 306, no. 1-2, pp. 71–82, 2005.

[17] V. B. Patravale, A. Date Abhijit, and R. M. Kulkarni, "Nanosuspensions: a promising drug delivery strategy," *Journal of Pharmacy and Pharmacology*, vol. 56, no. 7, pp. 827–840, 2004.

[18] E. Vega, F. Gamisans, M. L. García, A. Chauvet, F. Lacoulonche, and M. A. Egea, "PLGA nanospheres for the ocular delivery of flurbiprofen: drug release and interactions," *Journal of Pharmaceutical Sciences*, vol. 97, no. 12, pp. 5306–5317, 2008.

[19] J. Araújo, E. Vega, C. Lopes, M. A. Egea, M. L. Garcia, and E. B. Souto, "Effect of polymer viscosity on physicochemical properties and ocular tolerance of FB-loaded PLGA nanospheres," *Colloids and Surfaces B*, vol. 72, no. 1, pp. 48–56, 2009.

[20] K. Dillen, J. Vandervoort, G. van den Mooter, and A. Ludwig, "Evaluation of ciprofloxacin-loaded Eudragit RS100 or RL100/PLGA nanoparticles," *International Journal of Pharmaceutics*, vol. 314, no. 1, pp. 72–82, 2006.

[21] K. Dillen, C. Bridts, P. van der Veken et al., "Adhesion of PLGA or Eudragit/PLGA nanoparticles to *Staphylococcus* and *Pseudomonas*," *International Journal of Pharmaceutics*, vol. 349, no. 1-2, pp. 234–240, 2008.

[22] P. Costa and J. M. Sousa Lobo, "Modeling and comparison of dissolution profiles," *The European Journal of Pharmaceutical Sciences*, vol. 13, no. 2, pp. 123–133, 2001.

[23] J. Dai, T. Nagai, X. Wang, T. Zhang, M. Meng, and Q. Zhang, "pH-sensitive nanoparticles for improving the oral bioavailability of cyclosporine A," *International Journal of Pharmaceutics*, vol. 280, no. 1-2, pp. 229–240, 2004.

[24] D. Quintanar-Guerrero, E. Allémann, H. Fessi, and E. Doelker, "Preparation techniques and mechanisms of formation of biodegradable nanoparticles from preformed polymers," *Drug Development and Industrial Pharmacy*, vol. 24, no. 12, pp. 1113–1128, 1998.

[25] C. Vauthier-Holtzscherer, S. Benabbou, G. Spenlehauer, M. Veillard, and P. Couvreur, "Methodology for the preparation of ultra-dispersed polymer systems," *STP Pharma Sciences*, vol. 1, no. 2, pp. 109–116, 1991.

[26] J. Jaiswal, S. K. Gupta, and J. Kreuter, "Preparation of biodegradable cyclosporine nanoparticles by high-pressure emulsification-solvent evaporation process," *Journal of Controlled Release*, vol. 96, no. 1, pp. 169–178, 2004.

[27] L. A. Nkabinde, L. N. Shoba-Zikhali, B. Semete-Makokotlela et al., "Permeation of PLGA nanoparticles across different in vitro models," *Current Drug Delivery*, vol. 9, no. 6, pp. 617–627, 2012.

[28] J. T. S. Filho, R. D. Portugal, M. Loureiro, W. Pulcheri, and M. Nucci, "Characterization and analysis of the outcome of adults with acute myeloid leukemia treated in a Brazilian University hospital over three decades," *The Brazilian Journal of Medical and Biological Research*, vol. 44, no. 7, pp. 660–665, 2011.

[29] V. Hoffart, N. Ubrich, C. Simonin et al., "Low molecular weight heparin-loaded polymeric nanoparticles: formulation, characterization, and release characteristics," *Drug Development and Industrial Pharmacy*, vol. 28, no. 9, pp. 1091–1099, 2002.

[30] J. Vandervoort, K. Yoncheva, and A. Ludwig, "Influence of the homogenisation procedure on the physicochemical properties of PLGA nanoparticles," *Chemical and Pharmaceutical Bulletin*, vol. 52, no. 11, pp. 1273–1279, 2004.

[31] D. Zhang, T. Tan, L. Gao, W. Zhao, and P. Wang, "Preparation of azithromycin nanosuspensions by high pressure homogenization and its physicochemical characteristics studies," *Drug Development and Industrial Pharmacy*, vol. 33, no. 5, pp. 569–575, 2007.

[32] M. Kondo, T. Niwa, H. Okamoto, and K. Danjo, "Particle characterization of poorly water-soluble drugs using a spray freeze drying technique," *Chemical and Pharmaceutical Bulletin*, vol. 57, no. 7, pp. 657–662, 2009.

[33] P. Aksungur, M. Demirbilek, E. B. Denkbaş, J. Vandervoort, A. Ludwig, and N. Ünlü, "Development and characterization of cyclosporine A loaded nanoparticles for ocular drug delivery: cellular toxicity, uptake, and kinetic studies," *Journal of Controlled Release*, vol. 151, no. 3, pp. 286–294, 2011.

[34] Y. He, Y. Liu, Y. Liu et al., "Cyclosporine-loaded microspheres for treatment of uveitis: in vitro characterization and in vivo pharmacokinetic study," *Investigative Ophthalmology and Visual Science*, vol. 47, no. 9, pp. 3983–3988, 2006.